

## OPEN ACCESS

## EDITED BY

Gareth Perry,  
New Jersey Institute of Technology,  
United States

## REVIEWED BY

Denny Oliveira,  
University of Maryland, Baltimore County,  
United States  
Jean-Pierre Barriot,  
Geodesy Observatory of Tahiti,  
French Polynesia

## \*CORRESPONDENCE

A. Gordon Emslie,  
✉ [gordon.emslie@wku.edu](mailto:gordon.emslie@wku.edu)

†These authors have contributed equally to this work and share first authorship

RECEIVED 14 October 2025

REVISED 16 December 2025

ACCEPTED 22 December 2025

PUBLISHED 30 January 2026

## CITATION

Emslie AG, Hudson HS, Arbuckle G, Galloway JM, Peden T, May S, Ferguson T, Miller K, Cline T, Sawant S, Florence A, Gabbard K, Unseld J, Spalding L, Simpson M and Wright ET (2026) SunSketcher: a Citizen Science network project for the heliophysics big year.

*Front. Astron. Space Sci.* 12:1724714.  
doi: 10.3389/fspas.2025.1724714

## COPYRIGHT

© 2026 Emslie, Hudson, Arbuckle, Galloway, Peden, May, Ferguson, Miller, Cline, Sawant, Florence, Gabbard, Unseld, Spalding, Simpson and Wright. This is an open-access article distributed under the terms of the [Creative Commons Attribution License \(CC BY\)](https://creativecommons.org/licenses/by/4.0/). The use, distribution or reproduction in other forums is permitted, provided the original author(s) and the copyright owner(s) are credited and that the original publication in this journal is cited, in accordance with accepted academic practice. No use, distribution or reproduction is permitted which does not comply with these terms.

# SunSketcher: a Citizen Science network project for the heliophysics big year

A. Gordon Emslie<sup>1\*†</sup>, Hugh S. Hudson<sup>1,2,3†</sup>, Greg Arbuckle<sup>4</sup>, J. Michael Galloway<sup>4</sup>, Travis Peden<sup>4</sup>, Starr May<sup>4</sup>, Tameka Ferguson<sup>4</sup>, Kelly Miller<sup>4</sup>, Tabitha Cline<sup>5</sup>, Shikha Sawant<sup>4</sup>, Andrea Florence<sup>4</sup>, Kelcee Gabbard<sup>4</sup>, Janessa Unseld<sup>6</sup>, Leah Spalding<sup>5</sup>, Mark Simpson<sup>5</sup> and Ernest T. Wright<sup>7</sup>

<sup>1</sup>Department of Physics & Astronomy, Western Kentucky University, Bowling Green, KY, United States, <sup>2</sup>SUPA School of Physics and Astronomy, University of Glasgow, Glasgow, United Kingdom, <sup>3</sup>Space Sciences Laboratory, University of California, Berkeley, CA, United States, <sup>4</sup>School of Engineering & Applied Sciences, Western Kentucky University, Bowling Green, KY, United States, <sup>5</sup>Department of Art & Design, Western Kentucky University, Bowling Green, KY, United States, <sup>6</sup>Department of Psychological Sciences, Western Kentucky University, Bowling Green, KY, United States, <sup>7</sup>NASA Goddard Space Flight Center, Greenbelt, MD, United States

SunSketcher is an innovative program of eclipse observations that utilizes a network of smartphones along the path of totality to identify and geolocate the precise contact times via their definitive signature—Baily's Beads—and hence place meaningful constraints on the shape of the solar disk, in particular its oblateness. The common availability of GPS data for modern smartphones makes such an experiment possible. For the 2024 total solar eclipse in North America (a featured element of the Heliophysics Big Year), our program saw the successful development of the necessary smartphone app by a diverse team of undergraduate students at Western Kentucky University. The smartphone images *per se* are of rather low quality and not of first-order importance; the primary measurement is instead the precisely timed photometry during the second and third contacts, when the limbs of the Sun and Moon are nearly congruent and the Baily's Beads just appear. The app was downloaded by about 40,000 volunteers scattered along the eclipse path, from whom the program obtained about 100 GB of science-quality data. This article describes the status of our ongoing analysis of these data.

## KEYWORDS

apps and smartphones, citizen science (CS), oblateness, solar eclipse, timing

## 1 Introduction

This paper is dedicated to two of our late colleagues, Fred Espenak and Jay Pasachoff, whose inspiration and counsel were invaluable to the development and implementation of the SunSketcher project. We would have immensely enjoyed sharing these results with them.

In addition to the record closeness of the Parker Solar Probe to the Sun in December 2024, key elements of the Heliophysics Big Year (HBY) were the two solar eclipses that occurred during the HBY: the annular eclipse of 14 October 2023 and the total eclipse

of 8 April 2024, both visible from locations in the United States. The total solar eclipses of 2017 and 2024 provided North American observers with generally good conditions, and tens of millions of spectators, from eclipse enthusiasts to curious members of the public, admired the shows. They also provided an excellent opportunity for crowd-based observing programs, including those capable of serious scientific exploration. This article describes SunSketcher, a unique application of smartphone technology development aimed at using a network of smartphone timing observations to place constraints on the oblateness of the Sun.

The goals of SunSketcher were relatively straightforward:

1. Develop a smartphone app, for both Android and iOS devices, to automatically take images of Baily's Beads during the times of second and third contact that define the interval of totality;
2. Use the timing information on the Beads, obtained from a large number of phones spread along and across the eclipse path, together with accurate maps of the lunar limb, to determine the shape of the Sun to an unprecedented accuracy.

The scientific importance of measuring the oblateness of the solar disk lies in constraining models of flows in the solar interior and also in providing input to tests of various theories of gravity (see, e.g., [Rozelot et al., 2009](#); [Wang et al., 2023](#), and references therein). We would note that the SunSketcher goal *does not* involve measuring the absolute radius of the Sun, but rather the relative variation of it around the disk.

Our program grew out of the Eclipse Megamovie program ([Peticolas et al., 2019](#); [Hudson et al., 2021](#)) developed for the 2017 eclipse, and in 2024 we achieved a first success with this approach, utilizing a large outreach effort to achieve a first experiment, at scale, of a new kind of eclipse science. The project effort, supported by a grant from the NASA Heliophysics Innovation in Technology and Science (HITS) program, involved a team of faculty and students at Western Kentucky University. Under the collective direction of five faculty members, representing departments in both the Ogden College of Science and Engineering and the Potter College of Arts and Letters, the students worked synergistically to synthesize a variety of aspects of the project into a coherent effort, ever conscious of the absolutely immutable (astronomically-imposed) deadlines involved.

The app had to incorporate a variety of technical features, such as computation of eclipse ephemerides from interpolated tables of Besselian elements, determination of appropriate camera exposure settings, and data transfer protocols. In an effort to maximize participation, the app was intentionally designed to work completely independently "in the field"; no internet or phone connectivity was required to collect data (although download of the app and the subsequent data upload both had to occur through a US-based phone network). The necessary camera timings were informed by GPS timing and the exposure sequence ([Table 1](#) below) was hard-wired into the app software. In parallel, the app also involved a large measure of "User Experience" features designed to make the app appealing and straightforward to use ([Figure 1](#)) by untrained members of the public. Details on the development of the app can be found in [Galloway et al. \(2025\)](#). The project involved close liaison with several University entities, including Information Technology (the secure importing of data to a central server from a large collection of unverified phone IP addresses scattered across the eclipse path), the Institutional Research Board (Human Subjects

Research), and the Office of Legal Counsel (user privacy, issues related to collection of Personally Identifiable Information, Terms of Agreement, age restrictions, etc.). The success of the project was greatly enhanced through several external partnerships with the NASA Citizen Science and Education teams and with the SciStarter platform.

The critical beta-testing of the app was accomplished during the annular eclipse of 14 October 2023 at the University of Texas Permian Basin (UTPB) in Odessa, TX. This beta-test proved to be invaluable: it confirmed the camera timing driven by the local GPS phone position and the internally-stored eclipse ephemerides, it allowed different camera settings and exposure times<sup>1</sup> to be evaluated, and user surveys were conducted with UTPB staff and student volunteers to evaluate and subsequently improve the user experience. And, in a remarkably serendipitous event, WKU photographer Clinton Lewis took a series of images with a regular DSLR camera near the time of 3<sup>rd</sup> contact, and one of these images (used on the app home page; see [Figure 1](#)) showed a perfectly formed set of Baily's Beads in the portion of the occulted solar limb between the horns of the crescent Sun (see [NASA Science Editorial Team, 2024](#)). It subsequently proved relatively straightforward to identify the deep lunar valley<sup>2</sup> responsible for the brightest Bead, thus validating the underlying concept behind the SunSketcher project.

At the April 2024 total eclipse itself, every aspect of the program worked extremely well, although there were some inevitable glitches ([Galloway et al., 2025](#)). Despite some rather dismal cloud-cover forecasts, the sky condition all along most of the eclipse path turned out to be favorable for eclipse viewing and indeed the locations of the volunteer observers nicely map out the path of the eclipse, as shown in [Figure 2](#).

## 2 Data

### 2.1 Data structuring

Based on an interpolation of the Besselian elements for the eclipse, stored internally, the app calculated the eclipse timing for each individual observer's GPS location. Specifically it predicted, each to within an accuracy of a few seconds, the times of 2<sup>nd</sup> and 3<sup>rd</sup> contacts (hereafter C2 and C3, respectively) when the Baily's Beads would appear. The app then programmed the device's camera to obtain appropriate exposure sequences, each with an exposure time of 1/8000 s, according to the program cadence listed in [Table 1](#). This short exposure time, typically the shortest offered by the cameras,

- 
- 1 The planned exposure times were estimated *a priori* using test images of the full Moon, which coincidentally has an intensity close to that of the eclipsed solar corona. During the beta-test, a wide range of exposure times, close to those believed to be optimum, were used, and the images evaluated to arrive at the exposure time of 1/8000 s that was used for the actual total eclipse observations. The automated exposure feature for the smartphone camera had, of course, to be temporarily disabled by the app.
  - 2 tentatively named "Clinton Valley" by the team.

TABLE 1 Exposure sets.

Set	Number of exposures	Exposure time	Interval between exposures	Duration
		(seconds)	(seconds)	(seconds)
Pre-C2	5	1/8000	2.0	10
C2	40	1/8000	0.5	20
Post-C2	5	1/8000	2.0	10
Central	1	1/2000	-	-
Pre-C3	5	1/8000	2.0	10
C3	40	1/8000	0.5	20
Post-C3	5	1/8000	2.0	10
Total	101			

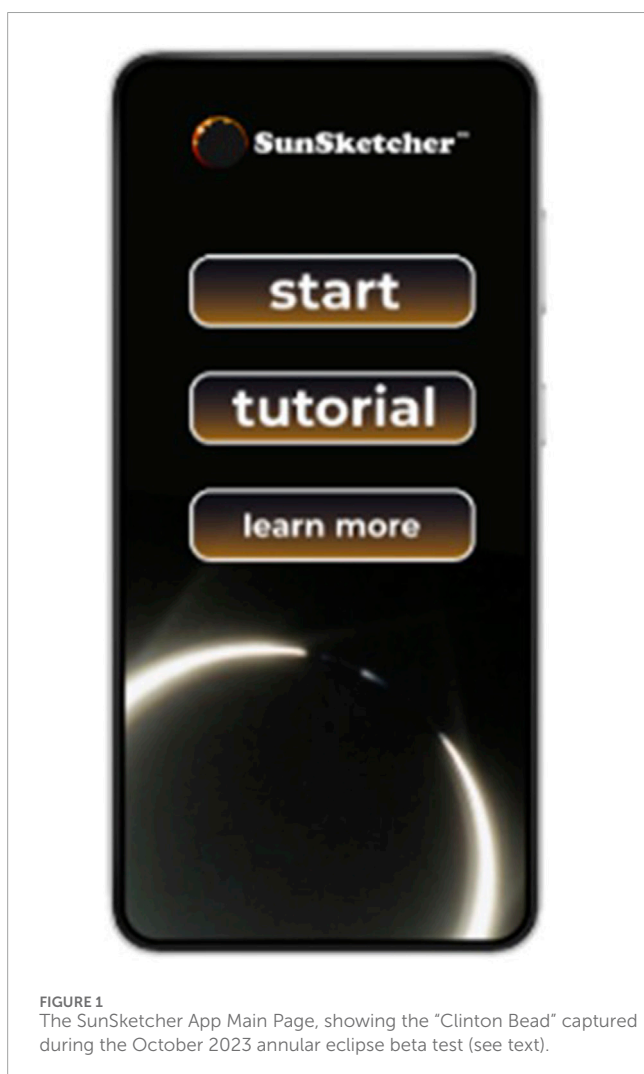


FIGURE 1  
The SunSketcher App Main Page, showing the “Clinton Bead” captured during the October 2023 annular eclipse beta test (see text).

satisfactorily exposed the fully eclipsed corona and provided a negligible amount of time for Bead distortion due to lunar disk motion across the Sun (in 1/8000 s the Moon moves a mere 15 cm or so). Only still images were taken, all in compressed format (.jpg).

The cadence pattern of the exposures initially reflected conservative thinking both about the accuracy of the ephemeris calculation and the nature of the camera behavior in the various smartphone architectures—the many different camera types for which the behavior could not be exactly anticipated. In order to ensure that the critical Baily’s Bead phases of the eclipse were captured, exposures commenced 20 s before each contact and continued until 20 s after that contact. Exposures started and ended with a 2 s cadence, but the cadence was increased, to 0.5 s between images, during the  $\pm 10$  s time interval centered on the contact time calculated from the ephemeris. This resulted in a total of 50 exposures at each contact. In hindsight, the long string of equally-spaced exposures both prior to and after each of the C2 and C3 contact times proved to be very valuable. While the C2 and C3 times calculated by the app were in fact accurate to within about one second, fitting polynomials to the photometric intensities of the sequence of images both before and after the contact time serendipitously provided, as we show below, much more precise times for the Baily’s Bead appearance/disappearance than could be obtained from the single exposure closest to that contact time.

To reduce the data volume associated with 100 full-frame smartphone images to a more manageable size, cropping of the images, necessarily performed within the smartphone itself prior to data upload, was required. This was carried out using an additional single (“Central” in Table 1) exposure taken during mid-totality with a significantly longer exposure time of 1/2000 s. The bounding box for the cropped area included a generous margin to allow for diurnal drift of up to one degree (2 solar diameters) during the  $\leq 4$  minutes of totality between the C2 and C3 sequences. The cropping process resulted in a minimalistic 5K size for each image, for a total

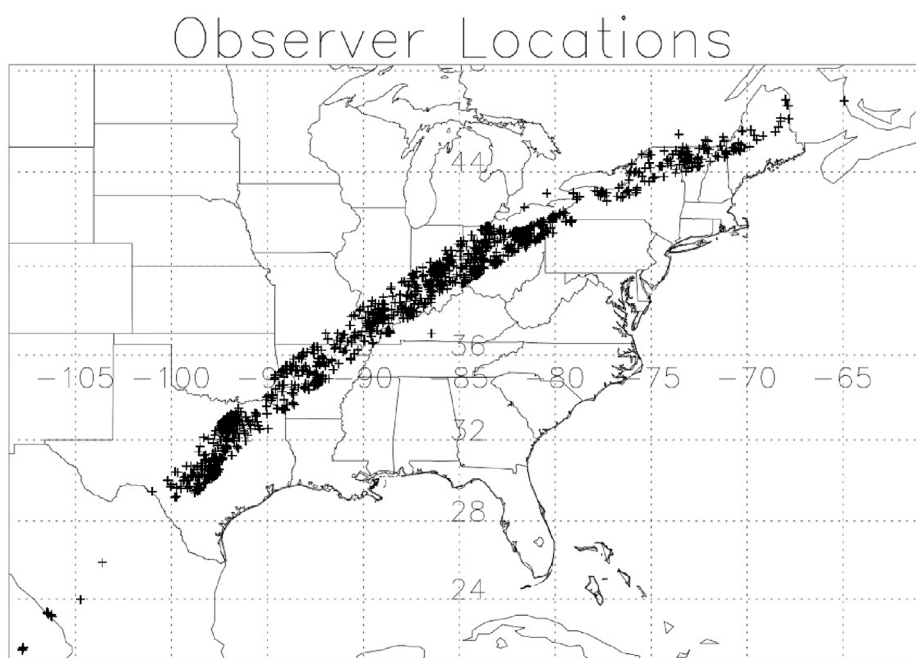


FIGURE 2

The geographical distribution of SunSketcher observers along the eclipse path. The self-contained nature of the app did allow observations to be taken outside the Continental US (e.g., the observations in [and off the coast of] Mexico and in Canada), but for privacy-related legal reasons, the download of the app and the subsequent data upload both had to occur through a US-based phone network. The gap in observations over upstate New York was due to a cloud layer that, unlike for many locations along the eclipse path, did not dissipate. The lone off-centerline “observation” in South Central Kentucky—the location of Western Kentucky University—was included in the database after the fact as an acknowledgment to the SunSketcher team.

download of a very manageable 0.5 MB for the entire collection of images. The cropping process also resulted in several different image pixelizations, depending on the individual camera type.

Nearly 40,000 app downloads (both iOS and Android combined) were performed. The app worked near-flawlessly in the field, and data were obtained from locations all along and across the eclipse path (see Figure 2). Over 200,000 cropped images, constituting about 100 GB of data, were uploaded to a server on the WKU campus and organized into searchable folders, which were shared with the Solar Data Analysis Center, together with a short instructional document.

In our processing, each user’s data (identified only by ID number and GPS information) constitutes a single .FITS file. Because of the legal requirement for anonymity, these files do not contain metadata beyond that actually written in the file name, which includes the GPS geolocation and timing, but not the phone number or its MAC address. Figure 3 shows three images from each of two observers (ID 1024 and ID 1033), showing good Bead exposures at both C2 and C3, and the central image used for image cropping.

These samples show that camera and image-cropping worked perfectly, and (as expected) the image quality is very poor; depending upon the camera type, the plate scale of such images is roughly  $0.1 R_{\odot}$  per pixel-width. (We would emphasize that this is not critical to the science objectives, which depend on precise *timing* of features, rather than precise *imaging* of the event). Since we did not require “attitude control” from the observers, we expect to find arbitrary azimuth angles and image inclinations in the data (cf. the  $\sim 40^{\circ}$  difference in the azimuthal orientations of the corona

that is apparent in the mid-totality images on the top and bottom rows of Figure 3). In order to provide a range of observing times for observers clustered in the same location, a random “jitter” in the range  $\pm 0.25$  second, equal to half the fastest image cadence (Table 1), was applied to the camera instructions in each phone.

## 2.2 Data acquisition volume

It is unclear how many users actively participated in eclipse observations, including those that did and did not successfully transfer data files. There are two metrics for the number of people who were attracted to the SunSketcher opportunity: the number of app downloads, and the ID counter of the SunSketcher server. The total number of app downloads was 35,323 (7723 Android and 27,600 iOS). Once one of those downloaded apps is actually opened, a user ID is assigned to the app, incrementing a global counter. The ID counter on the server was at approximately 32,000 at the start of the eclipse in the US, and rapidly increased throughout the day (even after the eclipse had concluded in the US!), reaching approximately 40,000 by the end of the day and eventually to 42,034 in total.

During the actual eclipse, 2,145 users successfully transferred some amount of data, although an unfortunate error in the logic regarding phone-server communications during the period of high server query rate immediately after the eclipse did result in some upload failures, as discussed by Galloway et al. (2025). The *average* (mean) number of images per user was 77.6, but the *median* turned out to be comfortably at the maximum possible value of 101,

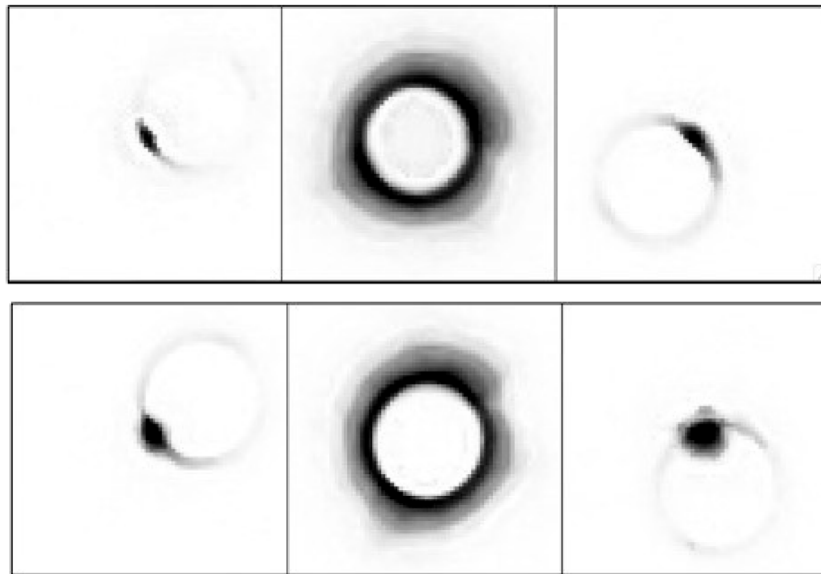


FIGURE 3

Sets of three representative images from two observers (top, ID 1033, and bottom, ID 1024). The three images are for C2 Bead, central, and C3 Bead, and Table 2 gives the metadata. The different geographical locations of the observers relative to the eclipse central line resulted in different azimuthal positions for the Bead appearances; the upper set is for an observer close to the eclipse centerline (near Greenwood, IN) while the lower set is for an observer offset to the northwest (near Dallas, TX).

TABLE 2 Sample metadata (central image).

Observer	Time (UT)	Latitude	Longitude	Altitude
	8-Apr-2024	(degrees N)	(degrees W)	(m)
ID 1024	18:42:33.127	32.865406	96.937767	23.7
ID 1033	19:08:10.652	39.657185	85.960335	207.7

indicating that the mean had been brought down by a few outliers that involved a very low number of transmitted images. To the surprise of some of the more skeptical members of the team, no data was received<sup>3</sup> showing pictures of the ground (phone oriented back-to-front) or of non-solar-eclipse-related (e.g., group picture, “selfie”) images. If a user’s app functioned as expected in one sense (data transfer), the app also generally worked in all other aspects (e.g., Sun in field of view, recorded location and time stamps on images) for that user. Most of the data was successfully transferred to the server within 48 h of the eclipse.

## 2.3 Image brightness variations

For a single observer, the light curves generated by the adopted image sequence result in characteristic patterns such as that seen in Figure 4. All brightness levels refer to a  $64 \times 64$ -pixel

box centered on the centroid location in the full image. Prior to the time of C2 contact at the beginning of totality, the overall intensity in the image decreases quite rapidly, as the visible area of solar disk decreases, the intensity variation then flattens considerably, reflecting the brightness of the solar corona. (The opposite is, of course, true around the time of the C3 contact at the end of totality, with a near constant intensity suddenly changing to a rapid increase as the solar disk emerges from behind the occulting lunar limb).

## 3 Assessment of data quality

The analysis concept for SunSketcher data depends strictly upon the timing of the key moments of the total eclipse, namely, second and third contacts. In principle none of the details of the observation (camera tilt or orientation, thin cloud, camera type, etc.) matter to first order, although of course they can play an important role in the form of background confusion by degrading the measurement. We can control this by data selection within our highly redundant database. The recording of both C2 and C3 by each observer is a crucial asset. We have conducted an initial simple analysis to assess the data quality, leading to the exploitation (Section 4) of the mathematics derived in Supplementary Appendices 1, 2, and

<sup>3</sup> The app did offer each user the opportunity to review the images prior to approving their upload to our server, and so it is possible that such images may well have been taken but not approved for upload by the user.

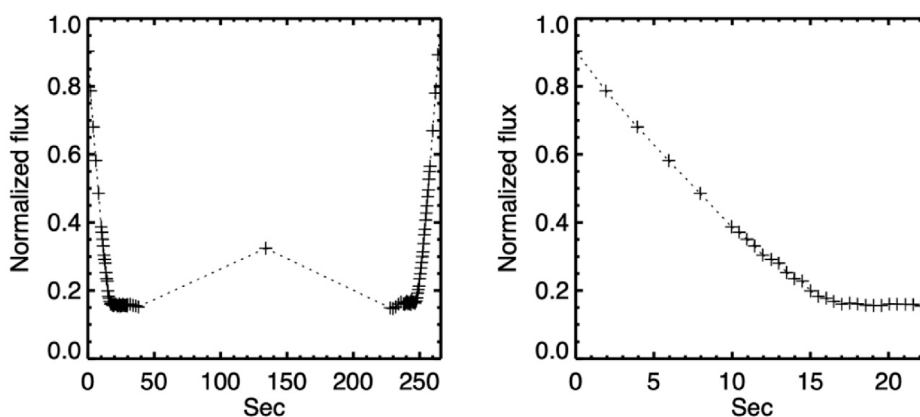


FIGURE 4

Light curve data for a single observer, showing raw signal totals for all images (left) and for the C2 disappearance (right). (Note the change in image cadence from  $\Delta t = 2$  s prior to  $t = 10$  s to  $\Delta t = 0.5$  s thereafter; see Table 1). The mid-totally image (at  $t = 140$  s in the left panel) has  $4 \times$  the exposure of that for the two contact epochs (see Table 1), and was used to identify the correct location in the camera field of view for image cropping. Note that the image totals here do not match the  $4 \times$  factor because they are from the raw JPEG data, including dark noise.

eventually to a full analysis incorporating the rough structure of the lunar limb (Section 5.1).

The basic analysis requires a definition of the Bead timing, and hence it is important to assess the ability of the SunSketcher data set to measure such timings to the precision required for a scientifically useful result. In Figure 5 we illustrate our basic scheme for this. This construction uses the intersection of two straight lines fitted to fixed ranges in the image sequence: (1) the blue sloping lines represent fits to the variation of intensity within the steep parts of the image dynamic range (which already includes saturated pixels) and so essentially reflects the growth of saturated area in the image, on time scales of a few seconds away from the actual Bead epoch, and (2) the horizontal thick red lines are linear fits to a range of images during the totality. For C2 the image ranges [24:28] and [33:37] for the outer (Bead) and inner (eclipse) fits, and for C3 the procedure was applied to image sets [67:71] (inner) and [76:80] (outer), where the frame numbers refer to the image sequence given in Table 1. We multiply the fitted value for totality (thick red line) by a factor of two to obtain the horizontal dotted red line, the intersection of which with the blue line defines the contact time prescriptively. Note that this calculation involves several *ad hoc* choices: for example, we arbitrarily took a fixed brightness level of twice that of the central image (the corona) for the red reference dotted horizontal lines. The intersection of the two lines does establish a precise time, as derived from the GPS data and the image brightnesses, but it also reflects systematic uncertainties due to the assumptions and can be substantially improved as we replace this approach with a better algorithm.

Figure 6 next analyzes the precision of the app's time reporting, based on the crude timing definition illustrated in Figure 5. The three datasets<sup>4</sup> have about 350 valid reports, from users spanning the full

hour of observations along the eclipse path from Texas to Maine (with an approximately 10-min-long gap around 19:20 UT, when totality was occurring over [cloud-covered] western New York State; see Figure 2). The scatter plots compare time differences between the measured C2 and C3 times and the ephemeris times as set in the app. These residuals are not centered on zero, which we explain as a combination of minor ephemeris errors in the app software and the differences between the “knee” times computed using the methodology illustrated in Figure 5 and the ephemeris contact time.

Table 3 gives the quantitative results for the three datasets. For each of the two contacts, we show  $N$ , the number of values used, the mean difference (s) between the contact times inferred using the methodology of the methodology illustrated in Figure 5 and the ephemeris contact times, and the standard deviation  $\sigma$  and standard error  $SE = \sigma/\sqrt{N}$  (both in s) of the time differences. Given the approximations made at this level of analysis, these results are very encouraging, inasmuch as the final standard error in the event timing is about 100 m. This level of precision, corresponding roughly to 100 m at the Moon and  $\sim 0.04$  Mm at the Sun, is already comparable to that of the best existing solar diameter determination (Brown and Christensen-Dalsgaard, 1998), and we expect major improvements as we sharpen the analysis. And, at this level of precision we have indeed entered the domain in which lunar limb structure will be detectable (see Figure 13 in Section 5 for a typical LOLA limb profile, where 0.1 arcsecond corresponds to  $\sim 200$  m on the Moon and  $\sim 70$  km on the Sun).

## 4 Full analysis: the lune model

Just at the point of contact, the brightness variation of a Bead (or set of Beads) can be complicated to understand. Encouraged by the quality of the data revealed by the basic analysis in Section 3, we therefore proceed, as a first approximation, to apply a basic “lune” model, which describes the variation of the brightness of an idealized solar crescent just before the C2 contact time or

<sup>4</sup> We identify these datasets based on the edge length (171, 417, 423) of the cropped image frames in pixel units. These different numbers of pixels presumably represent different smartphone types.

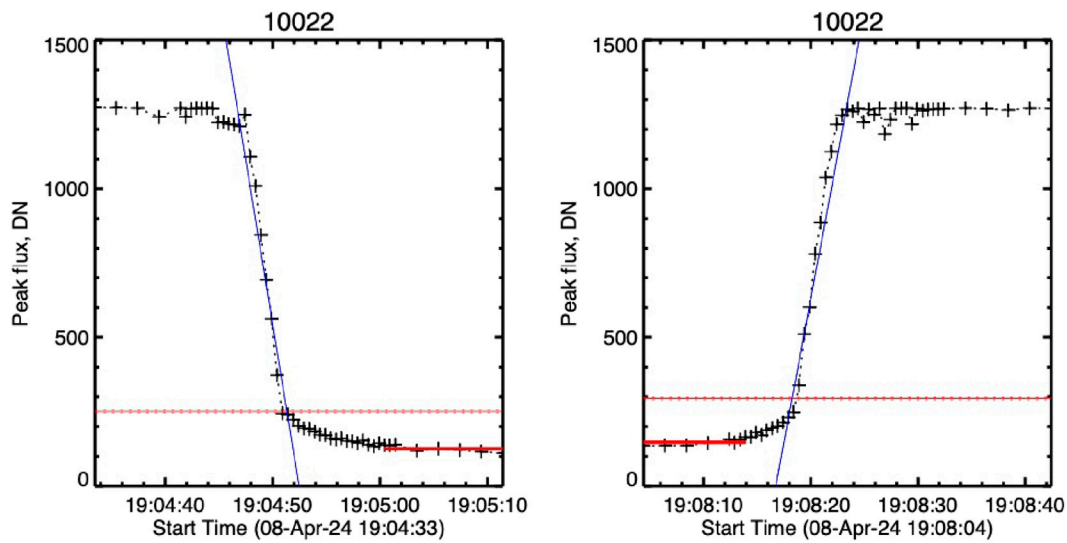


FIGURE 5

Illustration of the time estimation, via the intersections of linear fits to the brightness variations during the Bead phase, with a reference based on the signal level during the total eclipse. This shows the data of observer ID10022.

just after the C3 contact time, and we extend this model to the procedures necessary to achieve the SunSketcher science goal: a measure of the solar oblateness. This analysis improves the precision of the timing fits, and also allows us to distribute the observers' individual datasets to specific azimuthal locations around the limb of the Sun. Such an analysis, which intrinsically involves overlapping circular disks, cannot of course directly address the main science objective of determining the solar oblateness. However, as we shall see, it *can* be used to quantify the precision of the data set. As we shall see, the results are sufficiently encouraging to offer considerable promise that the science objective can indeed be obtained using a more advanced analysis that employs the LOLA lunar profile database (Section 5.1).

#### 4.1 Determination of “knee” times

As shown in Supplementary Appendix 1, the area (solid angle) of the exposed solar crescent is

$$A(t) \approx \left[ \frac{4\sqrt{2}}{3} \sqrt{\frac{ab}{b-a}} v^{3/2} \right] |t - t_c|^{3/2},$$

where  $a$  and  $b$  are the radius of the Sun and Moon, respectively (both in arc seconds),  $v$  (arcsec  $s^{-1}$ ) is the velocity of the lunar disk across the solar disk, and  $|t - t_c|$  represents the time before (C2) or after (C3) the respective contact.

The effective sizes of the solar and lunar disks  $a$  and  $b$ , and the relative velocity  $v$  of the two disks in the plane of the sky are known constants. Further, if the intensity is approximately constant for all points on the exposed solar crescent, the observed brightness (above background) is simply proportional to  $A(t)$ . Thus

$$I(t) = K_1 |t - t_c|^{3/2} + I_{b1}, \quad (1)$$

where  $I_b$  is a background intensity reflecting the remaining Bailey's Beads (see below), the exposed solar corona, and other sources of light (e.g., stars, planets, terrestrial sources, instrument dark background). Equation 1 is a simple empirical form with which the data for the steep sections of the intensity-time curves around the C2 and C3 contact times can be compared.

For the shallower portions of the intensity-time curve (when the solar crescent has become a series of Bailey's Beads), we could also model the intensity of an individual bead as that corresponding to the Sun sinking into (or rising from) a triangular-wedge-shaped lunar valley. It is easy to show that for such a geometry the area of exposed solar surface, and hence the amount of transmitted sunlight, varies approximately as the square of the distance between the limb of the Sun and the bottom of the valley, and hence as the square of the time difference relative to the time of contact. Therefore, the shallow portion of the light curves can be modeled with the parabolic form

$$I(t) = K_2 |t - t_c|^2 + I_{b2} \quad (2)$$

(solid red curves in Figure 5); this formula is most accurate when there is a single dominant bead present. The times  $t_k$  of the “knees” in the light curve (i.e., the intersection of the steep and shallow fits (2) and (3), measured on both sides of mid-totally) can be determined by equating expressions Equations 1, 2, giving the quartic expression in  $x = \sqrt{|t_k - t_c|}$ :

$$K_2 x^4 - K_1 x^3 - (I_{b1} - I_{b2}) = 0;$$

this could be used to improve on the values for for the two “knee times”  $t_k$ .

Figure 7 shows our application of this method (for simplicity, restricted just to the lune area term in Equation 1), applied to the same dataset as in Figure 5. This uses a time series mask function to cover progressive sequences of five images during C3 as given by the series  $\Delta t \times n^{1.5}$ , for integers  $n = [0, 4]$  (and the reverse sequence for

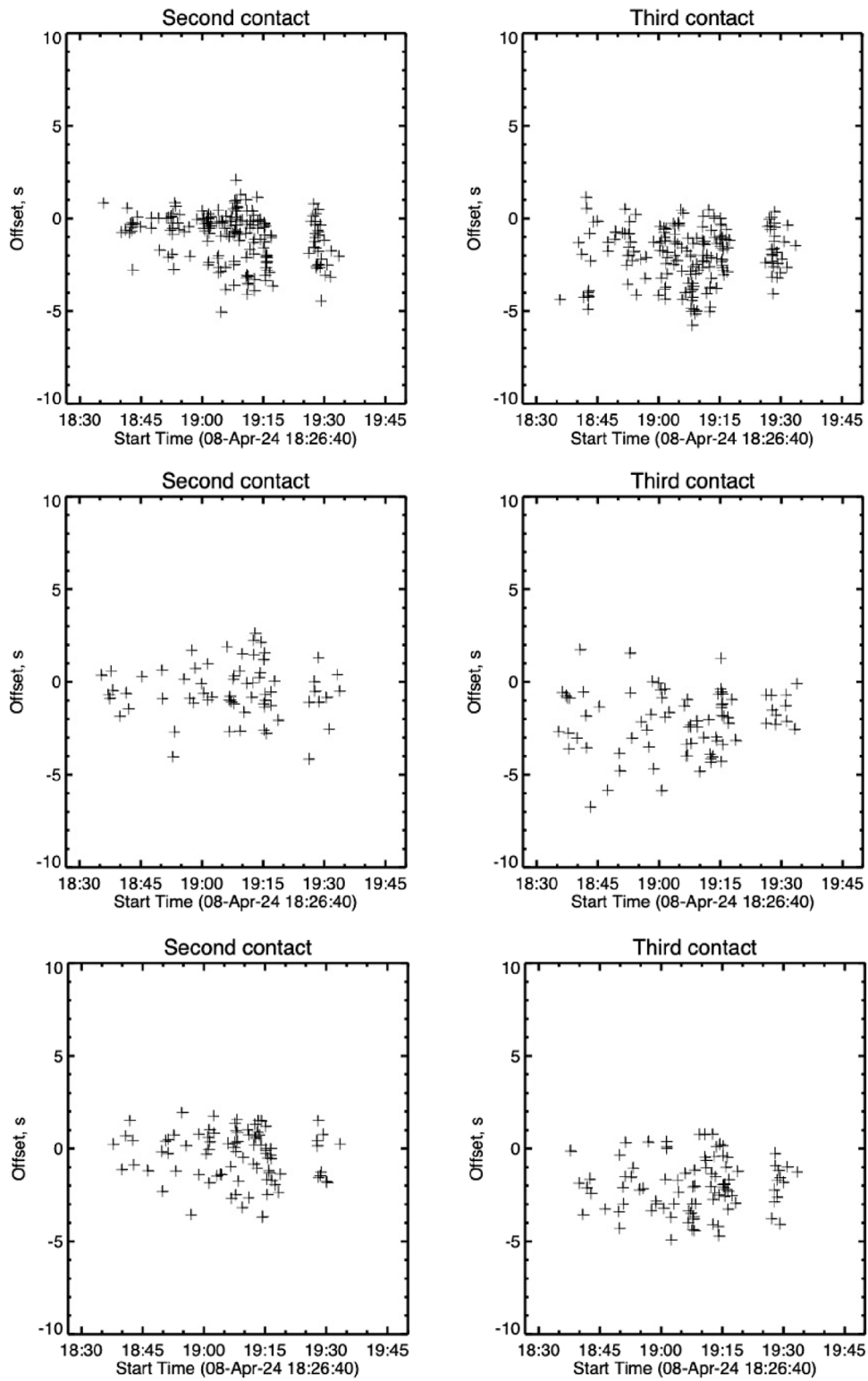


FIGURE 6  
 Timing discrepancies between the app predictions and the actual contact times obtained for each of the three main datasets of the 2024 data, based on the method of Figure 5. Top to bottom: Datasets 171, 417, and 423, labeled by their camera properties (see text).

TABLE 3 Timing results from the basic analysis.

Contact	Dataset	Number	Mean (s)	$\sigma$ (s)	SE (s)
Second	171	197	-0.983	1.275	0.091
	417	68	-0.447	1.422	0.174
	423	87	-0.399	1.361	0.147
Third	171	192	-2.048	1.460	0.104
	417	80	-2.141	1.649	0.201
	423	92	-1.999	1.406	0.152

C2), where  $\Delta t = 30$  s; this five-point correlation, applied to a span of  $4 \times \Delta t = 2$  minutes, along the observed data array (blue in the figure) maximizes at the position of the “knee” in the light curve. The red histogram in Figure 7 shows Gaussian fits used to the correlation function, the peaks of which can be used to obtain precise values for the “knee” times  $t_k$ . As shown in the next subsection, the collection of “knee times” for different observers are sufficiently precise to indeed be used to determine a first approximation to the solar disk shape.

## 4.2 Use of “knee” times to determine the solar oblateness

From the “knee” times determined by each observer, we can define that observer’s chord length  $\ell = (t_{C3} - t_{C2})$ , the time between the two “knee” times at the second and third contacts. The collection of such chords (one for each observer) all lie parallel to the direction of motion of the Moon (the  $t$ -direction); the ends of each chord are at the positions  $t_1$  and  $t_2$ , relative to the time of central totality on the centerline—the origin in Figure 8, and each chord is offset from the (maximal, central) chord by an amount that depends on the perpendicular distance  $y$  of the observer from the eclipse centerline (converted to time units by dividing by the speed of the Moon relative to the observer; see Supplementary Appendix 2). If we imagine each chord as a rod of length  $\ell$  parallel to the  $t$ -axis and placed at a distance  $y$  from the eclipse centerline, then the shape of the solar disk (size, oblateness, orientation of major axis) is in principle determined by the end points of this collection of rods (see Figure 8).

Supplementary Appendix 2 shows how to calculate the ellipse parameters in the general case. However, a considerable simplification results if we make the reasonable assumption that the major axis of the solar disk is approximately aligned with the eclipse centerline (this assumption is valid for the 2024 April eight eclipse, where the offset angle varies from about  $-18^\circ$  at the Texas/Mexico border to about  $-14^\circ$  in central Indiana to about  $-6^\circ$  in Eastern Maine (Jubier, 2024)), we obtain the simple result

$$\ell^2 = 4 \left( a^2 - \frac{y^2}{1 - e^2} \right) = 4 \left( a^2 - \frac{y^2}{(1 - f)^2} \right),$$

where  $e = \sqrt{1 - (b/a)^2}$  and  $f = 1 - (b/a)$  are the eccentricity and ellipticity of the solar disk. Because the maximum duration of totality varies along the eclipse track, the value of  $a$  is not unique and cannot be compared with accepted values of the solar radius. However, the variation of  $\ell^2$  with  $y^2$  is independent of the value of  $a$ , and hence the oblateness measure  $f$ , and its uncertainty, can in principle be determined from the best-fit slope  $d(\ell^2)/d(y^2)$  to the collection of  $(y^2, \ell^2)$  data points and its uncertainty  $\sigma$ :

$$f = \left[ 1 - \frac{2}{\sqrt{|d(\ell^2)/d(y^2)|}} \right] \pm \frac{\sigma}{|d(\ell^2)/d(y^2)|^{3/2}}. \quad (3)$$

Figure 9 shows the results obtained for the ‘171’ data set. The left panel shows the chord half-length vs. centerline distance. The points lie on a roughly circular band, as expected. The radius of the best-fit arc is 122 s, which agrees well with the 4 m 4 s duration of totality for centerline observers in the middle of the US section of the eclipse path. The considerable scatter above and below this arc is due to different durations of centerline totality, from a maximum of about 265 s (chord half-length 132 s) at the Mexican border to only  $\sim 200$  s (chord half-length 100 s) in Eastern Maine. There is a noticeable gap at a radius of  $\sim 110$  s, corresponding to the lack of observations over cloud-covered upstate New York, and there is also a considerable drop (Figure 2) in the number of observations to the East of this, i.e., with shorter totality durations/centerline chord lengths.

The right panel of Figure 9 shows the variation of the square of the chord distance  $\ell^2$  with the square of the centerline distance  $y^2$ ; the slope of the best fit line, and its uncertainty, are shown, and used in Equation 3 to determine the solar oblateness value  $f$  and its uncertainty.

The variation of the maximum duration of totality along the eclipse track, and hence the consolidation of the various individual measurements into a common framework, can be accommodated by normalizing all measurements to the duration of totality  $t_{\text{tot}}$  at the point on the eclipse centerline nearest the observer’s location (this was found using a quintic polynomial fit to the published (Jubier, 2024) values of totality duration at six locations along the eclipse centerline). Figure 10 shows the results obtained. While the scatter of Figure 9 has been reduced considerably and the gaps due to limited data have been eliminated, a considerable amount of scatter remains, and it becomes greater with off-centerline distance.

Figure 11 shows the distribution of the deviations of the chord half-lengths from the idealized circular fit line, normalized to the circular result; each panel also gives the value of the mean fractional deviation and its standard error. The scatter in the points becomes considerably larger at greater off-centerline distances, and the mean fractional deviation shifts to negative values. The number of observers with  $y > 0.4$  is less than 10% of the sample size and the data shows considerable scatter (cf. Figure 10). For this reason the histogram of results for such observers is not shown; however, the mean fractional deviation for such observers is  $0.25 \pm 0.06$ , a positive number that is clearly driven by the two points at very large  $y$  values (Figure 10). The exact cause of this very large discrepancy is not clear.

In addition, some measured chord lengths exceed the duration of totality at the proximate centerline location (left panel of Figure 10). These residual effects are presumably a consequence

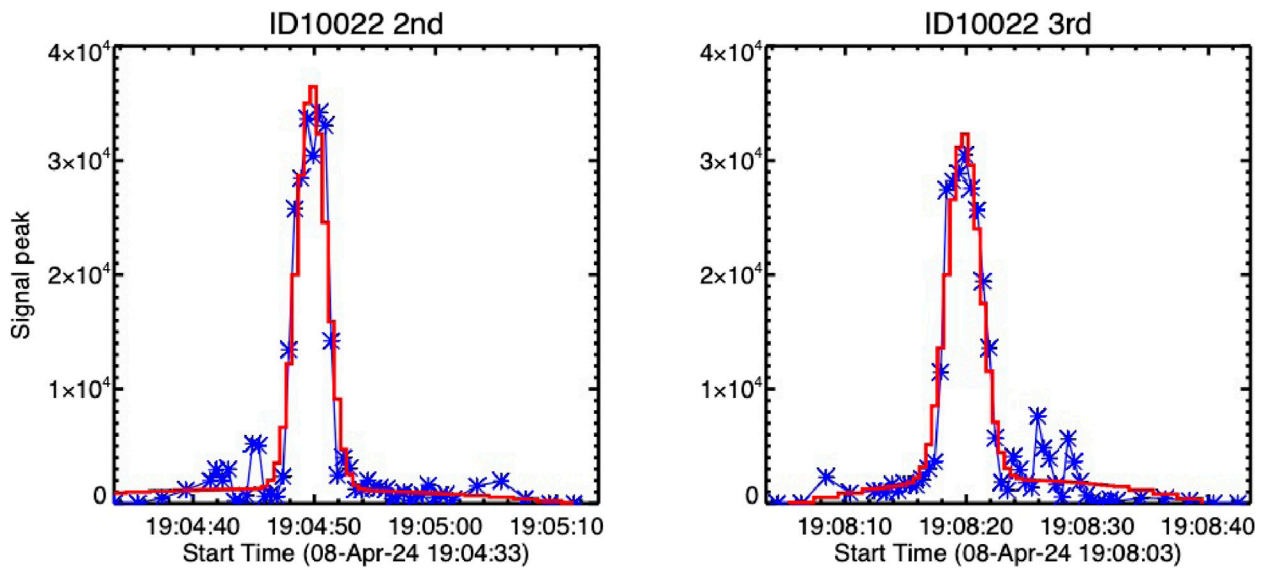


FIGURE 7

The same dataset as shown in Figure 5, but now with the masking against the prediction of the lune model as given in Equation 1. The blue points show the data correlated against this mask, with the mirror of the C2 mask applied to the C3 data. The red histograms are Gaussian fits from which the precise timings of the C2 and C3 “knees” are derived at the msec level.

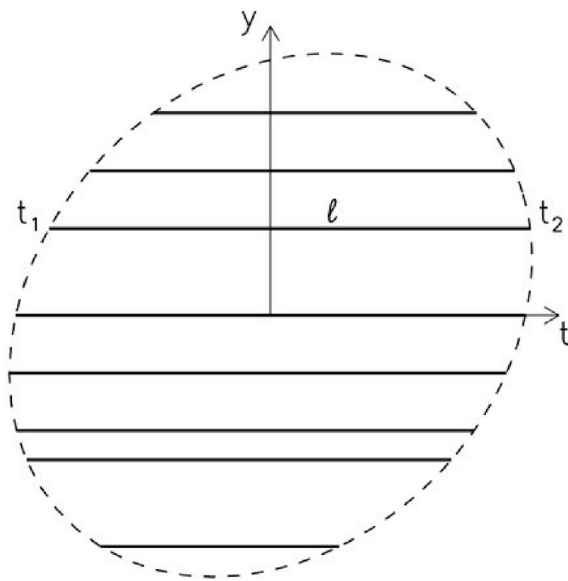


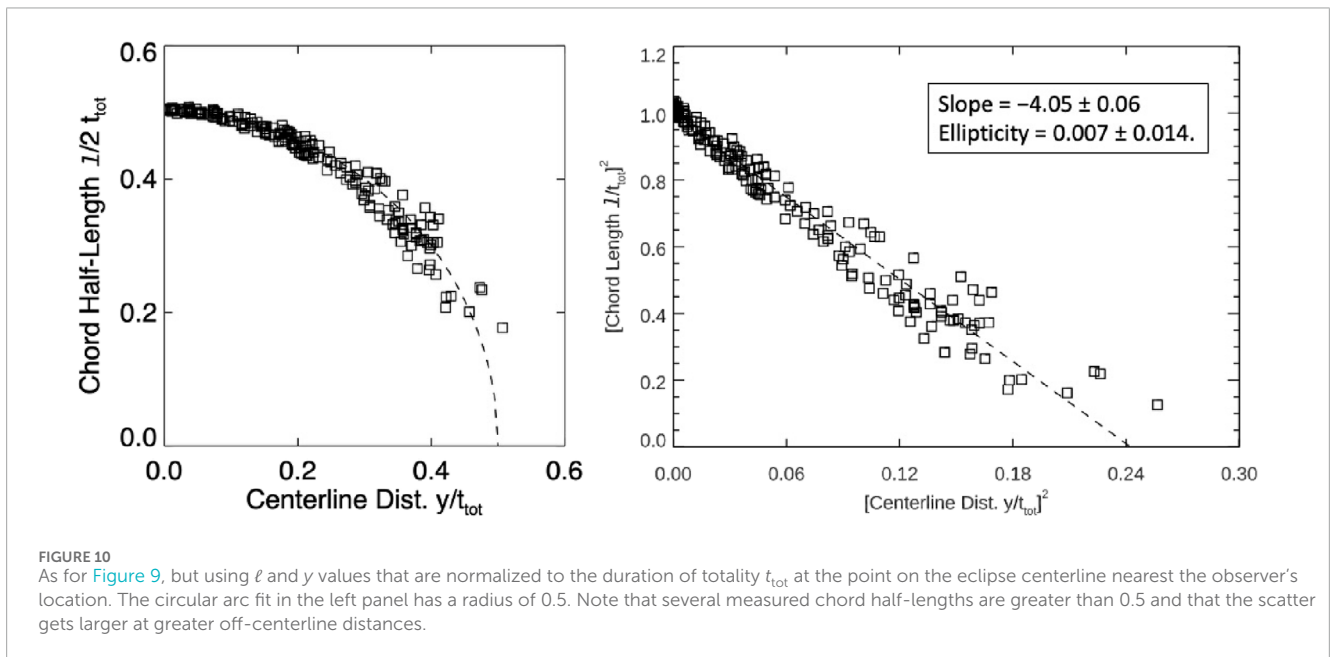
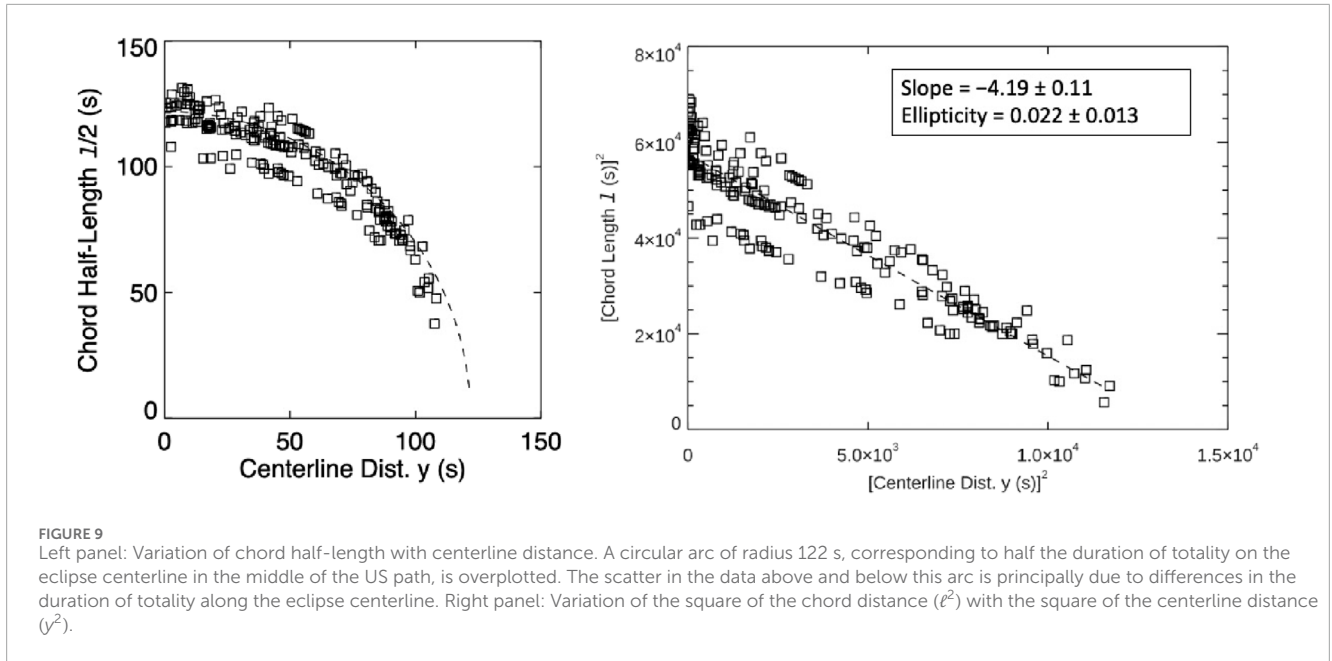
FIGURE 8

Schematic showing how combining the chord lengths for observers at various distances from the eclipse centerline can be used to determine the shape of the solar disk. A given observer is situated at a distance  $y$  from the eclipse centerline (the  $t$ -axis) and has a chord of length  $l$ , defined by the difference between the measured C2 and C3 contact times. The set of points defined by the ends of the chords  $t_1$  and  $t_2$  for different observers (Equation 6 of Supplementary Appendix 2) define the (elliptical) shape of the solar disk. In this example, the major axis of the ellipse is at  $45^\circ$  to the  $t$ -axis, so that the centers of the chords lie on a line of positive slope through the origin (Equation 10 of Supplementary Appendix 2).

of the way in which the C2 and C3 contact times, used to define the chord length, are calculated (Section 5). The resulting large uncertainty in the ellipticity (right panel of Figure 10), coupled with the numerous assumptions and approximations used to obtain even this zero-order result, reveals that an analysis that assumes a circular occulting disk is inadequate to provide a scientifically useful measure of the solar oblateness, even if allowance is made for the observer-dependence of the velocities used to convert off-centerline distance  $y$  to time units. On the positive side, however, the standard errors in the mean chord half-lengths shown in Figure 11 are of order a few thousandths of the centerline totality time. One thousandth of the centerline totality time is about 0.2 s, which corresponds to a lunar drift of about 200 m, or to a distance on the Sun of  $\sim 400$  times this, or 80 km. This is 1/10,000 of a solar radius, and comparable to the  $\sim 30$  km uncertainty in the best determination of the solar radius to date, obtained from solar meridian transit measurements (Brown and Christensen-Dalsgaard, 1998). We are therefore encouraged that the data is quite suitable for the application of a much more accurate methodology that uses the timing of individual beads relative to the mountain-and-valley structure of the lunar limb, as described in Section 5.1 below, and that such an analysis will indeed provide a scientifically useful measure of the solar oblateness.

## 5 Advanced analysis

The basic analysis described in Section 3 validated the SunSketcher concept, allowing us to assess the quality of the resulting data. The next step (Section 4) was to elaborate the complete “lune model” as described



in detail in [Supplementary Appendix 2](#). This approach should be considered as a reconnaissance based on mathematical first principles, and its further development will be valuable even though it does not incorporate the LOLA information we discuss below. The final analysis will incorporate this essential astrometric data to produce a best measurement of solar oblateness, the ultimate scientific goal of SunSketcher.

## 5.1 LOLA

While the analysis of the C2 and C3 contact times has been informative, a rigorous analysis of the data set must ultimately

use the Moon's figure as an astrometric reference. The precise geometry of the edge of the lunar figure can be obtained from the LOLA database, which derives its information from high-resolution images and global radar altimetry from the Lunar Orbiter Laser Altimeter (LOLA; [Smith et al., 2010](#)) instrument on the Lunar Reconnaissance Orbiter satellite. Incorporating the detailed shape of the occulting lunar figure into the analysis will allow direct comparisons of individual contact timings referred to the mask function provided by LOLA, using a parametrized solar shape (initially, an ellipse). In this section we provide some essential information about this approach. This final analysis thus differs from the reconnaissance we describe in this article. The final results will certainly be more precise, and probably limited eventually by

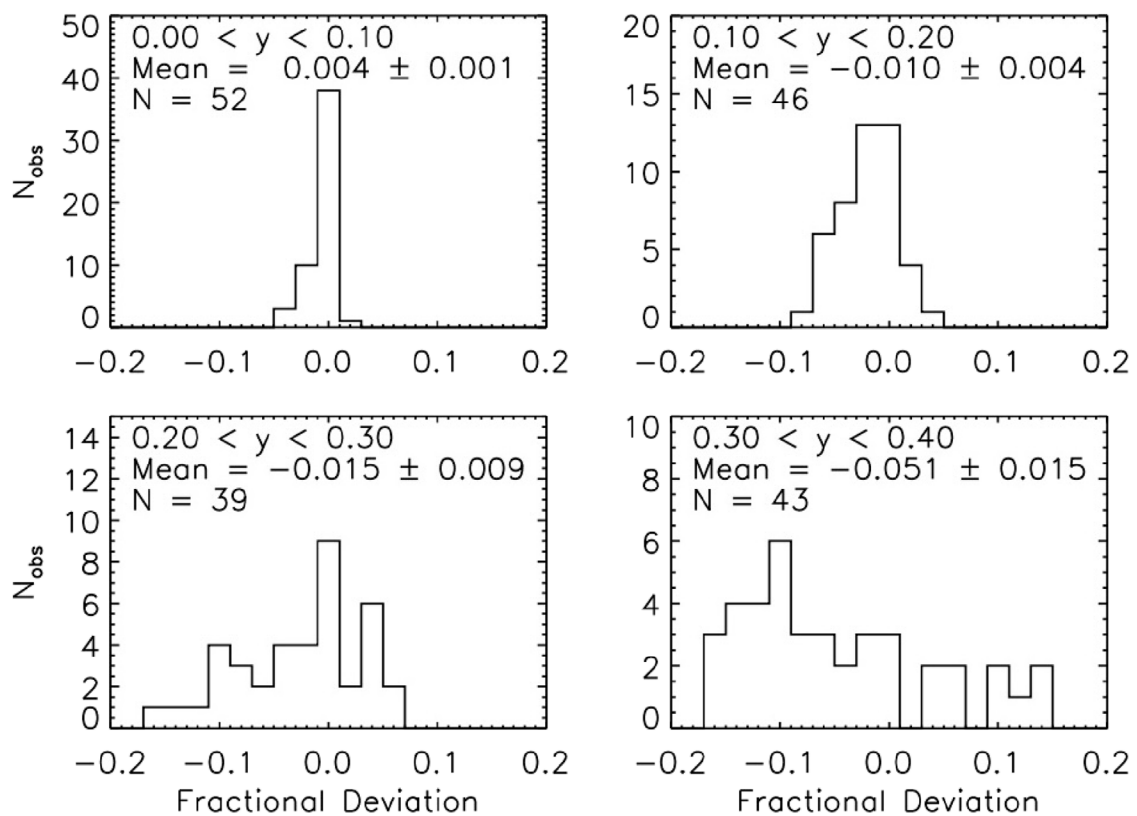


FIGURE 11

Histograms of the deviations of the chord half-lengths from the idealized circular arc profile (left panel of Figure 10). Results are shown for four groups of observers, with centerline distances  $y$  in bins of  $0.1 \times$  the duration of centerline totality. The abscissa bin size is  $\pm 0.01$ , and the bars are centered on integer multiples of  $0.02$ . The mean fractional deviation and its standard error, together with the number of observers in each sample, are shown in each panel.

systematic factors such as observer distribution and photometric precision.

The lunar orbit is not exactly circular, and the resulting variation in angular speed around its orbit means that its tide-locking to the Earth is not exact. This results in a slow *libration*, defined by two angular parameters. It follows that Earth-based observers at different times and locations will see a different configuration of lunar mountains and valleys around the limb. Figure 12 shows the LOLA database for a specific choice of libration angles (i.e., time and location of observation). Figure 13 shows the same limb-height map as in the right panel of Figure 12, but now with an array of observer locations at different locations relative to the eclipse centerline. The red asterisks mark the azimuth locations of Beads; because of parallax effects, the bead locations depend on the observer's position. The Figure shows a regular grid of hypothetical observers uniformly spaced in azimuth; for some subsets the Baily's Bead location will be redundant, with slight but significant differences not evaluated here. In general, the deeper the eclipse, the better the sampling.

The steps we envision consist of:

1. The development of a more sophisticated timing algorithm<sup>5</sup>, making use of just the data points within a second or so of the nominal ephemeris time, initially making use of the theoretical pattern developed in Section 2.3.
2. The generation of an eclipse ephemeris based on precise knowledge of the lunar limb, via the LOLA database information for each observer.
3. The optimization of a parametrized solar shape, considering (for example,) an ellipse defined by the three parameters  $[a, f, \theta]$  as described in Supplementary Appendix 2, evaluated for each observer's timing results.
4. Repetition of steps one to three, including the possibility of fine-tuning the ephemeris, to achieve the final value of  $f$  and its uncertainty estimate.

<sup>5</sup> The eclipse ephemeris loaded into the SunSketcher app was an approximate one, based on Besselian elements computed by our late friend Fred Espenak prior to the eclipse, and of course based on the assumption of a spherical Sun of nominal radius.

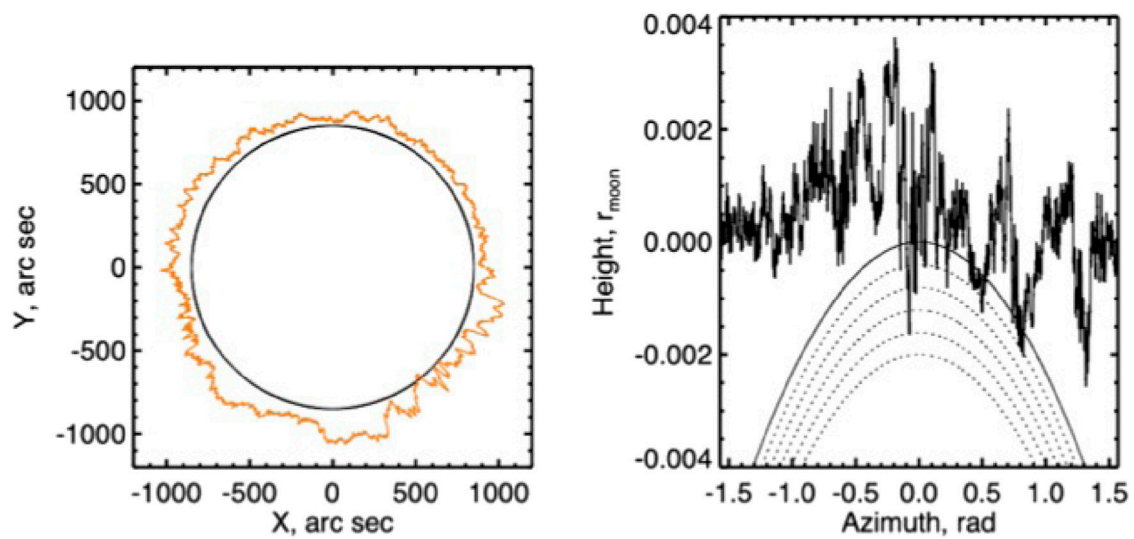


FIGURE 12

Two views of an example LOLA lunar limb: left, an exaggerated ( $1,000\times$ ) direct projection; right, polar coordinates (radial height vs. azimuth), showing how the solar disk (snapshots spaced at 1 s spacing) is sampled by differing lunar valleys to form Baily's Beads. For example, if the figure represents a C3 contact, with the disk of the Moon corresponding to the area below the lunar limb profile shown, then in the frame of the Moon, the Sun gradually intrudes from the bottom of the figure to the top, revealing more and more of the hitherto occulted solar disk. The first light to emerge is a single Baily's Bead corresponding to the deepest valley in the lunar limb profile at that azimuth (second to bottom solar limb profile shown). Over the next 2–3 s, an array of brightenings (e.g., the uppermost—solid line—solar limb profile) start to appear across a range of azimuths that is not necessarily centered on the initial “diamond ring” gleam. (For a C2 contact this sequence is, of course, reversed, with the solar disk profiles progressing from top to bottom, ending with a single bead of light that extinguishes at the onset of totality).

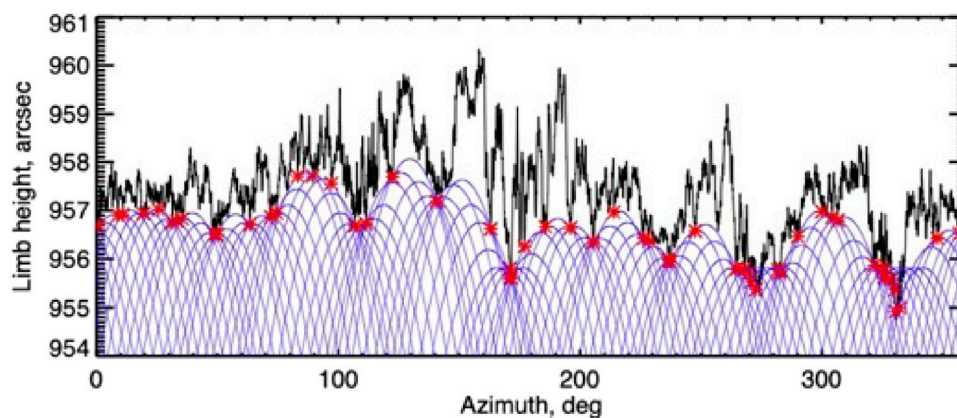


FIGURE 13

The blue curves show the different solar disk profiles as viewed, in the frame of the lunar limb at a specific time, by observers at different locations relative to the eclipse centerline. The red asterisks mark the positions of the Baily's Beads for each unique observer.

## 5.2 The solar radius

As noted in the Introduction, this article has *not* described a measurement of the solar radius, even though observers such as Jubier have already noted that Baily's Beads systematically appear at the “wrong” times, based on the IAU's established value (Prša et al., 2016) for this essential quantity. A precise confirmation of this point would probably require better optics and greatly improved image cadences. Further, any absolute determination of a best value for the solar radius must recognize the essential ambiguity in its definition, and the uncertainty of

fine-scale structure of the solar atmosphere as well. However, such considerations do not apply to the *relative* measures of the type we describe here, which explicitly aim at defining the *shape* of the Sun rather than its size.

## 6 Conclusion

As an outreach program, SunSketcher 2024 was a resounding success, involving thousands of active Citizen Science participants, fostering public awareness of heliophysics during the Heliophysics



FIGURE 14  
Future opportunities: the bands of totality for the total solar eclipses of 2026 August 12 (left), 2027 August 2 (middle) and 2028 July 22 (right).

Big Year, and inspiring a new generation of scientists and science enthusiasts. Scientifically, the method is sound, and a program incorporating a very large number of independent observers over a suitable time span has unique properties. Indeed, we had hoped for about a million observers during the very favorable 2024 eclipse, and although we fell well short of this goal, we nevertheless did acquire a great deal of science-quality data. Our data analysis of the 2024 eclipse is still in progress, so this article will not be the final report.

Lessons were learned that will allow us to extend and refine this approach in future eclipses, as described in the following section. In addition, we should consider a similar approach with GPS-equipped DSLR cameras, possibly extended to movie-format data. Such a program would trade off the sheer number of independent data sets in SunSketcher 2024 for vastly improved image resolution. A suitable camera would require a stable pointing mount (tracking not necessary), GPS, plus the ability to store the equivalent of the SunSketcher app to guide the image acquisition. Based on Figure 13, such a program would also require a reasonably large number of observers at different cross-track, locations.

## 7 The future

The data collected in 2024 represents but a single “snapshot” in the expected solar-cycle variation of the Sun’s shape. Continuations of the SunSketcher project will involve the eclipses of 2026 August 12 (Greenland, Iceland and Spain), 2027 August 2 (Gibraltar, Morocco, Algeria, Libya, Egypt, Saudi Arabia, and Yemen) and 2028 July 22 (Australia and New Zealand); see Figure 14.

For the 2026 eclipse, the track of totality covers mostly ocean or sparsely-populated regions, except for Northern Spain (where, however, the eclipse occurs very low in the sky, just before sunset). The associated challenges at mounting a large-scale Citizen Science effort are significant, and so instead efforts during this eclipse will focus on technology development. Team members familiar with the use of the app will use a basic version (with very limited User Experience functionality) to explore the use of DSLR cameras and/or movie-mode image sequences with improved time resolution. The data collected will be brought back to the US on the recording devices themselves, eliminating the need for remote data uploads and associated user privacy concerns.

The eclipse circumstances (e.g., solar altitude at mid-eclipse from observing sites on land) of the 2027 eclipse are considerably more favorable, and the significant amount of land coverage make a Citizen Science effort more feasible. While the basic functionality of the app will be essentially the same, a new set of challenges will appear. Lessons learned from 2024 and new phone camera technologies will be incorporated. The app will also need to be translated for users with native languages other than English and issues related to user privacy and the international transfer of data will need to be thoroughly addressed country-by-country.

The 2028 Australian eclipse offers the best opportunity to repeat the large-scale efforts of the 2024 eclipse, with the more advanced technologies and methodologies that will be available and/or developed by then. This eclipse has a totality path that includes the center of Sydney and several medium-sized (population 10,000+) towns in Western Australia and the Northern Territory, all within a 140-mile wide, 2000-mile long, path across a land mass where English is the primary language. Team members could be strategically deployed in sparsely-populated regions along the path of totality to fill in large gaps in the data coverage between the clusters of citizen scientists in the population centers of Western Australia and New South Wales. Partner institutions would be identified to assist in the aggressive publicity campaign necessary to produce a data set of sufficient quantity to meet the science goals—the single most important issue in 2024.

## Data availability statement

The datasets presented in this study can be found in online repositories. The names of the repository/repositories and accession number(s) can be found below: Solar Data Analysis Center.

## Author contributions

AE: Writing – review and editing, Formal Analysis, Funding acquisition, Writing – original draft, Project administration, Methodology, Conceptualization, Software, Investigation, Supervision. HH: Supervision, Conceptualization, Investigation, Methodology, Writing – review and editing, Software, Formal Analysis, Writing – original draft, Validation, Data curation.

GA: Conceptualization, Methodology, Investigation, Supervision, Writing – review and editing, Software, Funding acquisition, Project administration. JG: Methodology, Investigation, Data curation, Software, Supervision, Conceptualization, Writing – review and editing. TP: Investigation, Writing – review and editing, Methodology, Software. SM: Writing – review and editing, Data curation, Investigation, Methodology, Software. TF: Investigation, Writing – review and editing, Software, Methodology. KM: Methodology, Software, Investigation, Writing – review and editing. TC: Investigation, Writing – review and editing, Software, Methodology. SS: Methodology, Investigation, Software, Writing – review and editing. AF: Conceptualization, Methodology, Writing – review and editing. KG: Methodology, Conceptualization, Writing – review and editing. JU: Methodology, Conceptualization, Writing – review and editing, Software. LS: Methodology, Software, Supervision, Conceptualization, Writing – review and editing. MS: Supervision, Methodology, Writing – review and editing, Conceptualization, Software. EW: Investigation, Writing – review and editing, Software, Formal Analysis, Data curation, Methodology.

## Funding

The author(s) declared that financial support was received for this work and/or its publication. This work was supported by NASA Award 80NSSC23K1050 through the Heliophysics Innovation in Technology and Science (HITS) program. The WKU Extended Reality (XR) Lab, where most of this work was performed, was supported by the WKU Strategic Investment Fund and by the WKU Office of Research and Creative Activity.

## Acknowledgements

The various aspects of the SunSketcher project involved scores of individuals and groups along the way. The project brings to fruition ideas that originally were a part of the Eclipse Megamovie program of 2017, for which we acknowledge the support of Laura Peticolas, UC Berkeley, and Google. Jim Spadaccini and Ideum contributed a pioneering version of the app that was used in the 2017 and 2019 eclipses, which formed the initial basis for the app code used for SunSketcher. We also thank Xavier Jubier for the incredibly detailed Eclipse Maestro sites that greatly informed our efforts, and JPL Horizons for assistance with technical matters. We also thank the reviewers of the manuscript for very valuable suggestions that have significantly improved the manuscript.

We are pleased to acknowledge the immense efforts of, and hospitality offered by, Irene Perry and others at the University of Texas Permian Basin to facilitate the critical beta test of the app during the 2023 October 14 annular eclipse. We also express our appreciation to Lika Guhathakurta, Liz MacDonald, Kelly Korreck, Marc Kuchner and Michael Kirk at NASA for “buying into” the SunSketcher concept, featuring it as part of the Heliophysics Big Year, and helping to secure a meaningful volume of data by aggressively promoting SunSketcher through websites

and social media platforms. We thank Emma Giles at SciStarter for prominently including SunSketcher on their platform and hosting our networking website, and Sarah Kirn for her assistance with the Citizen Science aspects of the project. We would also like to acknowledge several individuals at WKU who provided support to the project in various ways. Lindsey Carter in the Office of Legal Counsel offered valuable advice regarding the various legal matters associated with anonymously collecting data from a large number of individual smartphones. The Associate Provost for Research and Creative Activity, Jenni Redifer, provided much needed resources to support the efforts of the growing cadre of student team members during the final phases of the project. Deans David Brown (Ogden College of Science and Engineering) and Terrance Brown (Potter College of Arts and Letters) pooled resources with those of the Office of Media Relations to purchase the SunSketcher T-shirts that were distributed to the team and also provided to various volunteers. University photographer Clinton Lewis lent technical and moral support and, through his expertly framed (and timed; see remarks in Section 1) photographs that were prominently featured on various websites, played a key role in alerting the public to the SunSketcher opportunity and in disseminating preliminary results. We would also like to thank the students who volunteered to be “test users” during the Google Play approval process for the Android app.

Last but by no means least, we thank the tens of thousands of members of the public who were sufficiently intrigued by the SunSketcher project to download the app and activate it during the 2024 total solar eclipse. While we (quite intentionally) do not know the identities of the individuals who supplied us with this unique data set, they themselves know who they are, and we are delighted to take this opportunity to offer our profound gratitude to all of them, to our team of SunSketcher Citizen Scientists. (And you all may wish to refer to this paper in your CVs).

## Conflict of interest

The author(s) declared that this work was conducted in the absence of any commercial or financial relationships that could be construed as a potential conflict of interest.

## Generative AI statement

The author(s) declared that generative AI was not used in the creation of this manuscript.

Any alternative text (alt text) provided alongside figures in this article has been generated by Frontiers with the support of artificial intelligence and reasonable efforts have been made to ensure accuracy, including review by the authors wherever possible. If you identify any issues, please contact us.

## Publisher's note

All claims expressed in this article are solely those of the authors and do not necessarily represent those of

their affiliated organizations, or those of the publisher, the editors and the reviewers. Any product that may be evaluated in this article, or claim that may be made by its manufacturer, is not guaranteed or endorsed by the publisher.

## References

- Brown, T. M., and Christensen-Dalsgaard, J. (1998). Accurate determination of the solar photospheric radius. *Ap.J. Lett.* 500, L195+–L198. doi:10.1086/311416500L.195B
- Galloway, M., Peden, T., May, S., Miller, K., Ferguson, T., Sawant, S., et al. (2025). “On development of sunsketcher: a heliophysics citizen science project,” in *Acmse 2025: proceedings of the 2025 ACM southeast conference southeast Missouri state university* (Cape Girardeau, MO, USA: Association for Computing Machinery), 95–104.
- Hudson, H., Peticolas, L., Johnson, C., White, V., Bender, M., Pasachoff, J. M., et al. (2021). The eclipse megamovie project (2017). *J. Astronomical Hist. Herit.* 24, 1080–1089. doi:10.3724/sp.j.1440-2807.2021.04.17
- Jubier, X. (2024). Eclipse circumstances for the 2024 April 8 total solar eclipse. Available online at: [http://xjubier.free.fr/en/site\\_pages/solar\\_eclipses/TSE\\_2024\\_GoogleMapFull.html](http://xjubier.free.fr/en/site_pages/solar_eclipses/TSE_2024_GoogleMapFull.html).
- NASA Science Editorial Team (2024). NASA’s scientists and volunteers tackle the October 14 solar eclipse. Available online at: <https://science.nasa.gov/get-involved/citizen-science/nasas-scientists-and-volunteers-tackle-the-october-14-solar-eclipse/>.
- Peticolas, L., Hudson, H., Johnson, C., Zevin, D., White, V., Oliveros, J. C. M., et al. (2019). “Eclipse megamovie 2017 successes and potential for future work”. *Celebrating the 2017 great American eclipse: lessons learned from the path of totality*. Editors S. R. Buxner, L. Shore, and J. B. Jensen (San Francisco: Astronomical Society of the Pacific), 516, 337.
- Prša, A., Harmanec, P., Torres, G., Mamajek, E., Asplund, M., Capitaine, N., et al. (2016). Nominal values for selected solar and planetary quantities: IAU 2015 resolution B3. *Astron. J.* 152, 41. doi:10.3847/0004-6256/152/2/41.15241P
- Rozelot, J. P., Damiani, C., and Pireaux, S. (2009). Probing the solar surface: the oblateness and astrophysical consequences. *Ap. J.* 703, 1791–1796. doi:10.1088/0004-637X/703/2/1791703.1791R
- Smith, D. E., Zuber, M. T., Jackson, G. B., Cavanaugh, J. F., Neumann, G. A., Riris, H., et al. (2010). The lunar orbiter laser altimeter investigation on the lunar reconnaissance orbiter mission. *Space Sci. Revs.* 150, 209–241. doi:10.1007/s11214-009-9512-y
- Wang, Y., Yan, J., and Barriot, J.-P. (2023). On the possibility of measuring solar flattening from photometry measurements taken during solar eclipses seen from the earth’s surface or Earth orbit. *Sol. Phys.* 298, 76. doi:10.1007/s11207-023-02172-z76W

## Supplementary material

The Supplementary Material for this article can be found online at: <https://www.frontiersin.org/articles/10.3389/fspas.2025.1724714/full#supplementary-material>